Check for updates

Article type : Regular Manuscript

TITLE: ELF18-INDUCED LONG NONCODING RNA 1 evicts fibrillarin from mediator subunit to enhance *PATHOGENESIS-RELATED GENE 1* (*PR1*) expression.

Jun Sung Seo[1], Piyarut Diloknawarit[1], Bong Soo Park[1], and Nam-Hai Chua[1,*]

[1] Temasek Life Sciences Laboratory, 1 Research Link, National University of Singapore, 117604, Singapore

[*] For correspondence (e-mail: bchcnh@nus.edu.sg; Tel: +65 68727001)

ORCID iD (Jun Sung Seo: 0000-0002-3420-8446; Bong Soo Park: 0000-0002-7726-2020; Nam-Hai Chua : 0000-0001-5931-3923)

Received: 19 July 2018

Accepted: 2 October 2018

Accepted Article

This is an Accepted Article that has been peer-reviewed and approved for publication in the *New Phytologist*, but has yet to undergo copy-editing and proof correction. Please cite this article as an "Accepted Article"; doi: 10.1111/nph.15530

This article is protected by copyright. All rights reserved.

Accepted Article

SUMMARY

- Plant immune response is initiated upon the recognition of pathogen-associated molecular patterns (PAMPs) such as elf18. Previously, we identified an Arabidopsis ELF18-INDUCED LONG NONCODING RNA 1 (ELENA1), as a positive transcriptional regulator of immune responsive genes. ELENA1 associated with Mediator subunit 19a (MED19a) to enhance enrichment of the complex on *PATHOGENESIS-RELATED GENE1* (*PR1*) promoter.

- *In vitro* and *in vivo* RNA-protein interaction experiments showed that ELENA1 can also interact with FIBRILLARIN 2 (FIB2). Co-immunoprecipitation (Co-IP) and bimolecular fluorescence complementation (BiFC) assay showed that FIB2 directly interacts with MED19a in nucleoplasm and nucleolus. Analysis of *fib2* mutant showed that FIB2 functions as a negative transcriptional regulator for immune responsive genes including *PR1*.

- Genetic and biochemical analyses demonstrated that ELENA1 can dissociate the FIB2/MED19a complex and release FIB2 from *PR1* promoter to enhance *PR1* expression.

- ELENA1 increases *PR1* expression by evicting the repressor (FIB2) from the activator (MED19a). Our findings uncover an additional layer of complexity in the transcriptional regulation of plant immune responsive genes by long noncoding RNA.

KEYWORDS

elf18, FIBRILLARIN 2 (FIB2), long noncoding RNA (lncRNA), mediator, *PATHOGENESIS-RELATED* GENE1 (*PR1*), plant innate immunity, pathogen-associated molecular pattern (PAMP), Arabidopsis

This article is protected by copyright. All rights reserved.

Accepted Article

INTRODUCTION

Immune responses of plants are initiated by the perception of pathogens via the recognition of conserved pathogen-associated molecular patterns (PAMPs) by plant pathogen- or pattern-recognition receptors (PRRs). PAMPs include bacterial flagellin, translation elongation factor Tu (EF-Tu), peptidoglycans, lipopolysaccharides, and fungal cell wall-derived chitin fragments (Jones & Dangl, 2006; Boller & Felix, 2009). Perception of different PAMPs by specific PRRs triggers innate immune responses that restrict pathogen propagation; this is designated as PAMP-triggered immunity (PTI) (Bigeard *et al.*, 2015). One of the best-characterized bacterial PAMPs is elf18 (Kunze *et al.*, 2004). Being derived from bacterial EF-Tu, it is recognized by the EF-Tu RECEPTOR (EFR) which is a member of the leucine-rich repeat (LRR)-RK family in Arabidopsis (Zipfel *et al.*, 2006). The ability to perceive elf18 seems to be restricted to Brassicaceae as other plant species can perceive EF-Tu via an epitope other than elf18 (Boller & Felix, 2009; Furukawa *et al.*, 2014). PAMP signals perceived by the PRRs are eventually transduced to the nucleus resulting in transcriptional changes of key genes, e.g. *PATHOGENESIS-RELATED GENE* (*PR*).

The traditional regulatory factors of transcriptional processes are mainly proteins but works done in the last two decades have provided evidence that RNAs can also function as important regulators as well. In particular, long noncoding RNAs (lncRNAs), which are so numerous in eukaryotes, have been implicated in many types of transcriptional regulation. lncRNAs may regulate transcription of their target genes through interaction with histone-modifying complexes, transcription factors (TF), Mediator complex and even RNA polymerase II (Lam *et al.*, 2014; Vance & Ponting, 2014; Long *et al.*, 2017). Different types of lncRNAs can be localized to different subcelluar compartments, such as nuclear, nucleolar, and cytoplasm. Information on the subcellular localization of a lncRNA is an important predictor of its function. For example, nuclear lncRNAs could plausibly be involved in direct transcriptional regulation; however, when a lncRNA is localized to the cytoplasm the possibility that the lncRNA may encode a short open reading frame that is translated should be considered (Batista & Chang, 2013; Chen, 2016). Some lncRNAs may function at the RNA level without interaction with any proteins, such as ribozymes or riboswitches. However, most lncRNAs execute their functions as ribonucleoprotein

This article is protected by copyright. All rights reserved.

particles (RNPs) (Cech & Steitz, 2014). In plants, analysis of over 200 Arabidopsis transcriptome data identified about 40,000 putative lncRNAs, including over 30,000 natural antisense transcripts (NAT) and over 6,000 lincRNAs (Liu *et al.*, 2012; Jin *et al.*, 2013; Wang *et al.*, 2014). So far, studies on individual plant lncRNA showed their involvement in gene silencing, flowering time control, circadian control, root development, photomorphogenesis, abiotic stress responses, reproduction, and innate immune response (Liu *et al.*, 2015; Henriques *et al.*, 2017; Seo *et al.*, 2017; Wang & Chekanova, 2017). However, molecular mechanisms of plant lncRNAs functions are still poorly understood, and only a few cases have been reported so far. IPS1 lncRNA carries sequence mismatches with miR399 and cannot be cleaved by the latter. It serves as a sponge for miR399 thereby reducing cleavage of the target *PHO2* mRNA (Franco-Zorrilla *et al.*, 2007). ASCO-lncRNA changes the splicing patterns of target mRNA by hijacking the nuclear speckle RNA binding proteins (NSRs), regulators of alternative splicing (Bardou *et al.*, 2014). COLDAIR, COLDWRAP, and COOLAIR lncRNAs are transcribed from *FLOWERING LOCUS C* (*FLC*) and function in *FLC* epigenetic silencing by recruiting the polycomb repressive complex (Liu *et al.*, 2010; Heo & Sung, 2011; Kim & Sung, 2017). Also, it was reported that the Antisense Long (ASL) transcript from *FLC* is involved in the maintenance of H3K27me3 to repress *FLC* expression (Shin & Chekanova, 2014). And very recently, AG-incRNA4, generated from the *AGAMOUS (AG)* second intron, represses AG expression through epigenetic silencing by associating with CURLY LEAF (CLF) (Wu *et al.*, 2018).

In eukaryotes, RNA polymerase II (Pol II) mediates transcription of all protein-coding genes. Pol II controls transcription of target genes through a combination of transcription activators and repressors to modulate the assembly and activity of the transcription machinery either by protein-protein interactions or by chromatin remodeling (Allen & Taatjes, 2015). Mediator (MED) complex functions as a transmitter or modulator between TFs and the basal transcriptional machinery, including Pol II and general TFs (GTFs), promoting the assembly of the pre-initiation complexes (PIC) on core promoters (Soutourina, 2018). Biochemical purification of the MED complex, along with protein sequence analyses, has identified Arabidopsis orthologs of all yeast and most human MED subunits; the Arabidopsis Mediator complex is composed of 28-34 subunits (Backstrom *et al.*, 2007; Bourbon, 2008).

This article is protected by copyright. All rights reserved.

Accepted Article

Mediator has become of increasing interest to plant science as it has been shown to be involved in the regulation of nearly all aspects of plant life, including development, flowering, defense, abiotic stress responses and metabolism (Samanta & Thakur, 2015; Dolan & Chapple, 2017).

Among nucleolar proteins (NOP), fibrillarin is an essential protein that has been conserved in its sequence and function throughout the evolution (Jansen *et al.*, 1991). This protein is a methyltransferase involved in the processing of the primary ribosomal transcript. It is mainly located in the fibrillar center (FC) and dense fibrillar component (DFC) region of the nucleoli where it is directly involved in several steps of ribosome biogenesis. Besides pre-rRNA processing, fibrillarin is implicated in several cellular processes including oncogenesis, viral progression, apoptosis, chromatin remodeling, basal transcription assembly, and transcription initiation suggesting it is active in subcellular locations other than the nucleoli (Rodriguez-Corona *et al.*, 2015; Shubina *et al.*, 2016). In plants, one of the fibrillarin proteins, FIBRILLARIN 2 (FIB2), has been found in association with the RNA Polymerase II transcription mediator complex as subunit 36a (Backstrom et al., 2007). So far, only a few studies about plant fibrillarin have been reported, and they are mostly related to pre-rRNA processing, viral progression and systemic trafficking in plants (Kim *et al.*, 2007; Chang *et al.*, 2016; Shubina *et al.*, 2016).

Previously, we have identified an Arabidopsis long-noncoding RNA (lncRNA), designated ELF18-INDUCED LONG NONCODING RNA 1 (ELENA1), as a positive regulator of expression of immune responsive genes. ELENA1 directly interacts with Mediator subunit 19a (MED19a) and promotes enrichment of MED19a, a positive regulator, on the *PR1* promoter (Seo *et al.*, 2017). Here, we show that MED19a could directly bind to FIB2 (MED36a), a negative regulator of *PR1* expression. Furthermore, ELENA1 can interact with FIB2 to dissociate the FIB2/MED19a complex. Taken together, our results provide further understanding of the regulatory mechanisms of the noncoding RNA, ELENA1, in immune responsive gene expression.

This article is protected by copyright. All rights reserved.

Accepted Article

MATERIALS AND METHODS

Plant materials, growth conditions, and treatment

Arabidopsis thaliana ecotype Columbia (Col-0), *med19a-1* (SALK_037435), *fib2-1* (SALK_022153) and *fib2-2* (SALK_093373) mutant plants were used. T-DNA insertion lines were obtained from the SALK collection. Homozygous plants for the T-DNA insertion were selected by genotyping progeny plants according to Alonso et al. (2003). The absence of target gene expression in homozygous plants was further confirmed by Real-time polymerase chain reaction (RT-PCR). Plants of all genotypes were grown on 0.6 % agar media containing 0.5 x Murashige and Skoog (MS) salts (MP Biomedicals), 1 % sucrose (Fisher) and 0.5 g/L MES hydrate (Sigma) in a growth room at 22 °C under 16 hr light/8 hr dark with white fluorescent light (~100 $\mu mol \bullet m^{-2} \bullet s^{-1}$). For elf18 (Axil Scientific) treatment, ten-day-old seedlings grown on MS solid medium were transferred to MS liquid medium (pH 5.7) with 1 % sucrose and 1 μM elf18 or flg22 and incubated under the same conditions. Seedlings were harvested at various time points after peptide application.

Generation of Transgenic lines

The m19a/fib2 double mutant was produced by genetic crossing between *med19a-1* and *fib2-1* knockout mutants. The M19a/fib2 lines were generated by transforming the *fib2-1* knockout mutant with *35S:GFP-MED19a*. The e1#10/fib2 line was produced by genetic crossing between *ELENA1* knock-down (KD) -10 and *fib2-1* knockout mutant. The E1/fib2 lines were generated by transforming *fib2-1* with *35S:-ELENA1* (Seo *et al.*, 2017). The entry clones of *FIB2* and *ELENA1* were recombined into pBA-DC and pER8-DC. Then we generated *35S:FIB2-myc* and *XVE:ELENA1/35S:FIB2-myc* transgenic lines using recombined constructs. P_{FIB2}*:FIB2-GFP* (P_{FIB2} : upstream 2 kb from *FIB2* start codon) plants were generated with pKGWFS7 vector (Karimi *et al.*, 2002). All constructs were verified by sequencing before being transformed into *Agrobacterium* strain GV3101. WT (Col-0) or mutant plants were transformed using the floral dip method (Clough & Bent, 1998; Zhang *et al.*, 2006).

This article is protected by copyright. All rights reserved.

Accepted Article

Real-time PCR Analysis

Total RNA was extracted from Arabidopsis seedlings using RNeasy plant mini kit (Qiagen) including DNase I treatment. Reverse transcription was performed using 2 µg of each total RNA and oligo $(dT)_{20}$ primers by the SuperScript III reverse transcriptase (Invitrogen). Real-time RT-PCR was performed using SYBR premix Ex Taq (Tli RNaseH plus) (TaKaRa) on the Bio-Rad CFX96 real-time system with gene-specific primers. Table S1 lists the primer sequences used.

Bacterial growth assays

Bacterial growth assays were performed as described (Katagiri *et al.*, 2002) with minor modifications. Overnight cultured cells of *Pseudomonas syringae* pv. *tomato* DC3000 were collected by centrifugation and washed. The cell pellet was re-suspended in water to $5x10^4$ colony-forming units (CFU)/ml. Arabidopsis leaves of 4-week-old plants were infiltrated with bacterial suspension using a needleless syringe. Four days after infiltration, leaf disks were ground in 100 µl H_2O, and serial dilutions were plated on King's B medium. Bacterial CFU was counted 2 days after incubation at 28 °C.

Recombinant Proteins and In vitro protein pull-down assay

The cDNAs encoding full-length MED19a and FIB2 were amplified by PCR and cloned into pENTR/D-TOPO vector (Invitrogen). MED19a and FIB2 entry clones were recombined into pGEX-DC-HA or pMAL-DC-myc by LR reaction. All constructs were transformed into *Escherichia coli* (BL21) strain, and each recombinant protein expression was induced by 0.5 mM isopropyl-b-D-thiogalactoside at 22°C overnight. Recombinant proteins were purified using glutathione-Sepharose 4 fast flow (GE Healthcare) or amylose resin (NEB) following manufacturer's instructions. To investigate MED19a interaction with FIB2, 500 µg glutathione S-transferase (GST)-MED19a-HA and 500 µg maltose binding protein (MBP) or MBP-FIB2-myc were mixed into 1mL of pull-down buffer (50 mM Tris-HCl, pH 7.5, 200 mM NaCl, 0.5 % Triton X-100, 0.5 mM beta-mercaptoethanol, and proteinase inhibitor cocktail) and

This article is protected by copyright. All rights reserved.

incubated at room temperature for 2 h. After incubation, reaction mixtures were pulled down with glutathione-Sepharose 4 fast flow (GE Healthcare) for 2 h and then washed five times with the same pull-down buffer. After washing, pulled-down proteins were separated on 10 % SDS-polyacrylamide gels and detected by immunoblotting using anti-myc antibody (Santa Cruz). ELENA1 and GFP RNAs were in vitro transcribed using MEGAscript T7 transcription kit (Thermo Fisher) treated with RNase-free DNase I (Invitrogen) and purified with RNeasy Mini Kit (Qiagen).

In vitro RNA pull-down assay

Biotin-labeled RNAs were in vitro transcribed using the Biotin RNA Labeling Mix (Roche) and T7 RNA polymerase (Roche), treated with RNase-free DNase I (Invitrogen) and purified with RNeasy Mini Kit (Qiagen). Nuclear extract was obtained from seedling samples as described (Heo & Sung, 2011). In addition, recombinant MED19a and fibrillarin proteins were expressed with pMAL-DC and purified using *E. coli* (BL21) expression system. 2 μg biotin-labeled RNAs and nuclear extract from *35S:GFP-MED19a* transgenic plants or recombinant MED19a and fibrillarin proteins were mixed in pull-down buffer (50 mM Tris pH 7.5, 150 mM NaCl, 2 mM DTT, 0.05 % NP-40 and protease inhibitor tablet (Roche)) and incubated for 6 hr at 4 °C. Thirty microliters of washed streptavidin agarose beads (Roche) were then added to each binding reaction mix and further incubated for 2 hr at 4 °C. Beads were washed briefly 5 times using binding buffer and boiled in SDS buffer. The supernatant was analyzed by Western blot using anti-GFP antibody (Santa Cruz).

RNA immunoprecipitation (RIP) assay

Two-week-old seedlings were harvested and cross-linked. Cross-linked samples were ground in liquid nitrogen, then resuspended in nuclei isolation buffer (0.44 M sucrose, 20 mM HEPES-KOH, pH 7.4, 10 mM $MgCl_2$, 1.25 % Ficoll, 2.5 % Dextran T40, 0.5 % Triton X-100, 8 U/ml RiboLock (Thermo-Fisher), 1 mM PMSF, 1 % Plant Protease Inhibitor cocktail (Sigma)), and the suspension was filtered with Miracloth. The crude nuclear fraction was centrifuged at 4,000g for 10 minutes at 4 °C. Each

This article is protected by copyright. All rights reserved.

Accepted Article

pellet was resuspended in nuclei lysis buffer (50 mM Tris-HCl, pH 8.0, 150 mM NaCl, 10 mM EDTA, 1 % SDS, 1 mM PMSF, 160 U/ml RiboLock, 1 tablet of Roche protease inhibitor cocktail) and the lysate was sonicated. Sonicated lysates were centrifuged at 15,000 g for 15 minutes at 4 °C. Supernatants were transferred to new tubes and 50 µl protein A agarose beads were added (Roche). After rotating the samples for 30 minutes at 4 °C, protein A agarose beads were pelleted. The supernatant was diluted to 1 ml with dilution buffer (1.1 % Triton X-100, 1.2 mM EDTA, 16.7 mM Tris-HCl, pH 8.0, 167 mM NaCl, 40 U/ml RiboLock, 1 % Plant Protease Inhibitor cocktail). Anti-myc antibody was added and the mixture was incubated overnight at 4 °C. Samples were sequentially washed using low-salt, high-salt, LiCl, and TE buffers (pH 8.0). To each sample was added 100 µl elution buffer (1 % SDS, 0.1 M $NaHCO_3$, 40 U/ml RiboLock), and samples were incubated for 10 minutes at room temperature. The elution step was repeated once. Eluted samples were treated with 20 µg proteinase K and incubated for 1 hour at 42 °C. To reverse cross-link, each sample was treated with 10 µl 5 M NaCl and incubated for 1 hour at 65 °C. RNA was purified using TRIzol (Invitrogen). After treatment with Turbo DnaseI (Ambion), RNA was used for first strand cDNA syntheses using oligo dT primers (Gene Link) with the Superscript III system (Thermo-Fisher). ELENA1 levels were normalized to levels of ACT2 mRNA. qRT-PCR reactions were performed on the Bio-Rad CFX96 real-time system. Primer sets used for qRT-PCR analyses are listed in Table S1.

BiFC and TriFC assay

Binary gateway bimolecular fluorescence complementation (BiFC) vectors were as described (Seo *et al.*, 2017). Using entry clones of *MED19a* and *FIB2*, we made BiFC constructs by LR reaction and used them for transient assays in *Nicotiana benthamiana*. In the case of trimolecular fluorescence complementation (TriFC) assay, full-length entry clones carrying *FIB2* and *MSCP* were recombined with BiFC vectors by LR reaction. Entry clone of *ELENA1* was recombined into p35S-GW-6xMS2 by LR reaction (Schonberger *et al.*, 2012). All constructs were transformed into Agrobacterium strain GV3101 using freeze and thaw method. Cultured cells were harvested and resuspended in 10 mM $MgCl_2$ plus 150 µM acetosyringone

This article is protected by copyright. All rights reserved.

Accepted Article

(Aldrich) and then kept at 25 °C for at least 3 hr without shaking. Agrobacterium suspensions were infiltrated into leaves of *N. benthamiana* with a needleless syringe. Leaf cells were analyzed using LSM 510 laser scanning confocal microscope (Zeiss) 2 - 3 days after the infiltration. Detailed procedures of TriFC assays were described in Seo and Chua (2017).

Antibody production and in vivo coimmunoprecipitation (Co-IP)

DNA fragment encoding MED19a full-length protein was amplified by PCR. The PCR product was inserted into pET-28a expression vector (Novagen) at the BamHI and XhoI sites. Proteins were expressed using *E. coli* (BL21) expression system and purified with ProBond^{TM} purification system (Novex). Polyclonal antibodies were raised against the purified His-MED19a protein in rabbits (ProfSci) and antibodies purified from serum were used in the western-blot analysis. For in vivo Co-IP, two-week-old seedlings of *35S:FIB2-myc* or *XVE:HA-PUB10/35S:FIB2-myc* treated with/without 1 μM elf18 or 20 μM beta-estradiol (Sigma-Aldrich) were ground in liquid nitrogen and homogenized in IP buffer (50 mM Tris-HCl, pH 7.5, 100 mM NaCl, 10 mM $MgCl_2$, 0.1 % Nonidet P-40, 1 mM PMSF, 10 % glycerol, 1 mM DTT, 50 mM MG132, and protease inhibitor cocktail). After centrifugation, the supernatants were used for IP. Input controls were taken for immunoblot analysis. An aliquot of the supernatant containing 1 mg total protein was precleared by adding protein A-agarose (Millipore), and the mix was incubated for 1 h before being centrifuged at 15,000 g for 1 min. The supernatant was incubated with the anti-myc polyclonal antibody (Santa Cruz) at 4 °C for 2 h. Antigen-antibody complexes were pulled down by protein A agarose at 4 °C for 2 h and washed five times with IP buffer. Immunoprecipitated proteins were eluted by boiling at 95 °C for 5 min in 23 NuPAGE LDS sample buffer (Life Technologies). Eluted proteins were separated on 12 % SDS-polyacrylamide gels and then transferred to polyvinylidene fluoride (PVDF) membranes (Millipore). Immunoblot analysis was performed with purified anti-MED19a polyclonal antibodies and anti-rabbit horseradish peroxidase-linked sheep antibody (GE Healthcare). Immunoblot signals were detected by Clarity^{TM} Western ECL substrate (Bio-Rad).

This article is protected by copyright. All rights reserved.

Accepted Article

Accepted Article

Chromatin Immuno-precipitation (ChIP) assay

ChIP assays were performed as described previously (Bowler *et al.*, 2004). After chromatin isolation, immunoprecipitation was performed using anti-c-myc (Santa Cruz). Cross-links were reversed by incubation at 65 °C for 12 hr, and DNA was purified with QIAquick spin columns (Qiagen) and eluted in 50 µl of Tris-EDTA (pH 8.0). Real-time quantitative PCR (RT-qPCR) was used to quantify the enrichment of different fragments on the *PR1* promoter. Firstly, relative enrichment of each fragment was calculated based on comparison to qPCR using input control. Secondly, relative enrichment was calculated by comparison to the control region. RT-qPCR reaction was performed on Bio-Rad CFX96 real-time system. Primer sequences are given in Table S1.

RESULTS

ELENA1 Interacts with FIB2

Previously, we reported that ELENA1 could directly associate with MED19a and promote enrichment of this mediator subunit on the *PR1* promoter to enhance its expression in Arabidopsis (Seo et al., 2017). We screened for possible binding of ELENA1 to additional mediator subunits using in vitro RNA binding assays. We found that FIB2 (*AT4G25630*) was able to bind to ELENA1 in vitro (Fig. 1A). Further binding competition assays with non-biotinylated RNA confirmed that the binding of ELENA1 to FIB2 was specific (Fig. 1B). To further examine the binding specificity between ELENA1 and the native FIB2 protein, we prepared nuclear extracts from *35S:FIB2-myc* transgenic lines and assayed its binding to in vitro transcribed ELENA1 RNA. We detected FIB2 association only with the sense (+) strand of ELENA1 (Fig. 1C), demonstrating the strand-specific interaction of ELENA1 with native FIB2-myc.

We checked in vivo association of sense ELENA1 with FIB2 using TriFC assay (Seo and Chua, 2017). We observed that the sense (+) strand of ELENA1 associated with FIB2 in the nucleus, but not the anti-sense (-) strand of ELENA1. Magnified YFP image showed that ELENA1 associated with FIB2 in both nucleolus and nucleoplasm (Fig. 1D). We also examined in vivo association of ELENA1 with

This article is protected by copyright. All rights reserved.

FIB2 after elf18 treatment by RIP assay using the *35S:FIB2-myc* lines and anti-c-myc antibody. Indeed, we were able to retrieve ELENA1 from FIB2-myc immuno-precipitates, and moreover, the association of ELENA1 with FIB2 was increased during elf18 treatment, as with MED19a (Fig. 1E). Taken together, these results provide further evidence that ELENA1 is specifically associated with FIB2 in vivo.

fib2 mutant Shows Altered Responses to *Pst* DC3000 and Enhanced Expression of Immune Responsive Genes

The FIB2 protein can be divided into four domains; glycine-arginine rich domain (GAR) domain, space region (SP), central domain with the RNA binding region, and alpha helix-rich domain (AHR). A methyltransferase domain is located through the central and AHR region (Fig. 2A)(Loza-Muller *et al.*, 2015). To investigate the function of FIB2 in plant innate immunity, we obtained T-DNA insertion mutants alleles (*fib2-1*; SALK_022153 and *fib2-2*; SALK_093373) from the SALK collection (Fig. 2A). To confirm the knockout (KO) mutants, we checked the *FIB2* transcript levels in KO mutants and marker gene expression in genomic complementation lines (Fig. S1). The results showed that *fib2-1* and *fib2-2* are indeed KO mutants of *FIB2*. We inoculated *fib2* mutant plants with *Pseudomonas syringae* pv *tomato* DC3000 (*Pst* DC3000) to examine defense phenotypes. Bacterial growth assays showed that KO mutant lines were more resistant to *Pst* DC3000 (Fig. 2B). Analysis of defense phenotypes of KO mutants showed that FIB2 is a negative regulator of resistance against *Pst* DC3000.

We also examined the expression of immune responsive genes, *PATHOGENESIS-RELATED GENE 1* (*PR1*; *At2g14610*), *CYTOCHROME P450, FAMILY 82, SUBFAMILY C, POLYPEPTIDE 2* (*CYP82C2*; *At3g57240*), and *ACIREDUCTONE DIOXYGENASE 3* (*ARD3*; *At2g26400*), investigated in our previous ELENA1 work (Seo et al., 2017). After 1 μM elf18 treatment, *PR1* expression level was higher in *fib2* mutants compared to WT at 12 hours and 24 hours (Fig. 2C). Also, *CYP82C2* and *ARD3* expression levels were higher than those of WT at both time points (Fig. 2D and 2E). Overall, our results show that FIB2 is a negative regulator of expression of immune responsive genes, including *PR1*, and of resistance against a bacterial pathogen.

This article is protected by copyright. All rights reserved.

Accepted Article

Accepted Article

FIB2 interacts with MED19a

FIB2 has been previously characterized as a component of the mediator complex, MED36a, in Arabidopsis (Backstrom et al., 2007). We use in vitro pull-down assays to examine possible interaction between MED19a and FIB2. Fig. 3A shows that the negative controls (GST and GST-MED28 resins) were unable to pull down MBP-FIB2, whereas MBP-FIB2 was efficiently retained by the GST-MED19a resin, suggesting that MED19a physically interacts with FIB2 in vitro. We also used yeast two-hybrid assay (Y2H) to investigate the interactions of MED19a with FIB2. GAL4 DNA-binding domain (BD) was fused to FIB2 and GAL4 activation domain (AD) was fused to MED19a and MED28. The negative controls (empty and MED28) were not able to survive whereas yeast transformed with MED19a and FIB2 was able to survive in selective media (Fig. 3B). Our Y2H results imply that MED19a physically interacts with FIB2.

We generated three independent *35S:FIB2-myc* transgenic lines, which showed different *FIB2* expression levels (Fig. S2A). To investigate the effects of *FIB2* transcription levels on *PR1* expression, we checked *PR1* expression levels after elf18 treatment. We found that different transcript levels of *FIB2* in *35S:FIB2-myc* lines did not affect *PR1* expression level (Fig. S2B). Next, we performed Co-IP using *35S:FIB2-myc* transgenic line to test FIB2/MED19a interaction in Arabidopsis cells. To detect MED19a protein in Arabidopsis, we generated rabbit polyclonal antibody against the native MED19a (Fig. S3). After protein extraction from *35S:FIB2-myc* transgenic line, we immunoprecipitated FIB2-myc proteins using anti-c-myc antibody. Proteins in the immune-complexes were separated on SDS-PAGE and immunoblotting with anti-MED19a antibodies detected the presence of MED19a in the immunoprecipitate (Fig. 3C). We further adopted BiFC assays to verify interactions of FIB2 with Med19a in planta. The N-terminal fragment of the yellow fluorescent protein (nYFP) was fused with MED19a and FIB2 was fused with the C-terminal fragment of YFP (cYFP). nYFP-MED19a was transiently co-expressed with FIB2-cYFP in *Nicotiana benthamiana* leaves. We found that the co-expression of nYFP-MED19a with FIB2-cYFP resulted in a strong YFP fluorescence in the nucleus of epidermal cells of *N. benthamiana* leaves (Fig. 3D), whereas no YFP fluorescence was detected in negative controls (nYFP-MED19a or FIB2-cYFP coexpressed with cYFP or nYFP). A magnified YFP image showed that the FIB2/MED19a complex

This article is protected by copyright. All rights reserved.

was located in the nucleolus as well as the nucleoplasm (Fig. 3D). Taken together, all the results consistently demonstrate that FIB2 directly interacts with MED19a in vitro and in vivo.

ELENA1 disrupts FIB2/MED19a complex

To investigate the effect of ELENA1 on FIB2/MED19a interaction, we applied in vitro pull-down assays using ELENA1, FIB2, and MED19a. GST-MED19a were incubated with MBP-FIB2 under different concentrations of ELENA1 RNA (or GFP mRNA). GST-MED19a and associated MBP-FIB2 were then separated on SDS-PAGE for immunoblotting with the anti-MBP antibody. As shown in Fig. 4A, GFP mRNA (right panel) which served as a negative control had little effect on FIB2/MED19a interaction, whereas ELENA1 (left panel) efficiently inhibited the interaction between FIB2 and MED19a proteins. These results suggest that ELENA1 physically blocks the interaction of FIB2 with MED19a in vitro.

Next, we performed Co-IP assay using *35S:FIB2-myc* transgenic line to study changes in FIB2/MED19a interaction after elf18 treatment in vivo. After 1 μM elf18 treatment, seedling samples were prepared in a time course experiment. After protein extraction from *35S:FIB2-myc* samples, we immunoprecipitated FIB2-myc using anti-c-myc antibody and the immune complexes were separated on SDS-PAGE for immunoblotting with anti-MED19a antibody. Fig 4B shows that the MED19a protein amount in complex with FIB2 was gradually reduced after elf18 treatment but the interaction of MED19a with FIB2 was not changed without elf18 treatment

We generated two independent *XVE:ELENA1/35S:FIB2-myc* transgenic lines (Fig. S4A). To investigate the effects of transgenic plants on *PR1* expression, we checked *PR1* expression levels after elf18 treatment. The result showed no difference in *PR1* expression levels of two independent transgenic lines compared to WT (Fig. S4B). Using *XVE:ELENA1/35S:FIB2-myc* transgenic lines, we further performed a Co-IP assay to check the effect of ELENA1 on FIB2 interaction with MED19a in vivo. After 20 μM beta-estradiol (inducer) treatment, seedling samples were prepared in a time course experiment. After protein extraction from the

This article is protected by copyright. All rights reserved.

Accepted Article

samples, we immunoprecipitated FIB2-myc proteins using anti-c-myc antibody and then separated on SDS-PAGE for immunoblotting with anti-MED19a antibody. The immunoblotting result also showed that the MED19a protein amount interacting with FIB2 was gradually reduced after induction of ELENA1 transcription, but no change in FIB2/MED19a interaction was seen in the absence of the inducer (Fig. 4C and Fig. S4A). Taken together, in vitro pull-down assays and Co-IP assays consistently show that ELENA1 disrupts the interaction of FIB2 with MED19a. On the other hand, *PR1* transcript levels were not changed even after beta-estradiol induction of ELENA1 (Fig. S4D). This result suggested that although ELENA1 could dissociate the FIB2/MED19a complex this lncRNA alone could not induce *PR1* expression in the absence of elf18-mediated signal transduction.

Roles of ELENA1, MED19a and FIB2 in *PR1* Expression

To investigate the relationship among ELENA1, MED19a, and FIB2 in *PR1* expression, we generated four different double transgenic lines of *ELENA1*, *MED19a*, and *FIB2*; *med19a-2*/*fib2-1* (m19a/fib2), *35S:GFP-MED19a*/*fib2-1* (M19a/fib2), *ELENA1* KD (knock-down) #10/*fib2-1* (e1#10/fib2), and *35S:ELENA1*/*fib2-1* (E1/fib2) (Fig. 5 and Fig. S6) (Seo *et al.*, 2017). We analyzed *PR1* expression in plants of the four genotypes after elf18 treatment. The m19a/fib2 mutant showed reduced *PR1* expression compared to *fib2-1* but higher *PR1* expression than that of *med19a-2* (Fig. 5A). Plants of M19a/fib2 lines showed enhanced *PR1* expression compared to *fib2-1* and M19a line (Fig. 5B). These results suggested that FIB2 represses MED19a activation function in *PR1* expression and that the dissociation of FIB2 from MED19a is important for full activation of *PR1* expression after elf18 treatment.

The e1#10/fib2 line showed reduced *PR1* expression compared to *fib2-1* but slightly higher *PR1* expression than that in e1#10 (Fig. 5C). Reduced *PR1* expression of the e1#10/fib2 line compared to *fib2-1* suggested that ELENA1 is required for the full activation of *PR1* expression. Furthermore, a higher *PR1* expression of e1#10/fib2 compared to e1#10 line suggested that removal of the FIB2 repressor from the FIB2/MED19a complex by ELENA1 is also required for the activation of *PR1* expression. The E1/fib2 lines showed enhanced *PR1* expression

This article is protected by copyright. All rights reserved.

Accepted Article

compared to *fib2-1* but a similar level of *PR1* expression compared to E1 line (Fig. 5D). A higher level of *PR1* expression of E1/fib2 suggested that ELENA1 has an activation function in addition to its role in removing the FIB2 repressor. Moreover, a similar level of *PR1* expression in E1/fib2 compared to *ELENA1* overexpressing (OX) lines suggested that ELENA1 already fully removed FIB2 and that E1/fib2 was a phenocopy of E1 OX. The results in Fig. 5C and 5D suggested that ELENA1 has dual functions: releasing the FIB2 repressor from the FIB2/MED19a complex and activating *PR1* expression. We have previously verified that ELENA1 activation function is closely related to MED19a enrichment on the *PR1* promoter (Seo *et al.*, 2017). Taken all the results of the double mutants together, we conclude that under elf18 treatment, ELENA1 promoted *PR1* expression by removing the repressor (FIB2) and activating positive regulators, including MED19a.

ELENA1 Promotes FIB2 Release from the *PR1* Promoter

To investigate the possibility of FIB2 release from the *PR1* promoter, we performed ChIP assays with P_{FIB2}*:FIB2-GFP* transgenic line. After the ChIP assays, we quantified the enrichment of 5 different regions (P1 to P5) on the *PR1* promoter by qPCR (Fig. 6A). FIB2 enrichment on the *PR1* promoter was decreased after elf18 treatment. FIB2 enrichment was the lowest at 12 hours after elf18 treatment and then reduced over 24 hr after elf18 treatment (Fig. 6B). FIB2 enrichment was higher in the P2, P4, and P5 regions than those of the other regions. This result demonstrated the reduced occupancy of FIB2 on the *PR1* promoter region during elf18 treatment.

To examine FIB2 enrichment in *ELENA1* mutants, we performed ChIP assays with P_{FIB2}*:FIB2-GFP*/*ELENA1* KD and P_{FIB2}*:FIB2-GFP*/*ELENA1* OX transgenic line. In *ELENA1* KD lines, the enrichment of FIB2 on the P4 region of the *PR1* promoter was increased compared to WT after elf18 treatment. On the other hand, the enrichment of FIB2 in the *ELENA1* OX line was lower than that shown in WT even without treatment and greatly decreased compared to WT (Fig. 6C). These observations are consistent with elevated levels of *PR1* transcript in *ELENA1* OX lines and reduced levels of *PR1* transcript in *ELENA1* KD lines during elf18

This article is protected by copyright. All rights reserved.

Accepted Article

treatment. These results support the view that ELENA1 facilitates the release of FIB2 from the *PR1* promoter.

DISCUSSION

Previously, we screened a group of Mediator subunits with high probable RNA binding motif (Seo et al., 2017), and among which was FIB2. ELENA1 specifically bound to FIB2 protein in vitro (Fig. 1A to C) and in vivo (Fig. 1D and E). Fibrillarin is a major nucleolar protein whose amino acid sequence and biological function have been conserved amongst eukaryotes. This protein is known to be mainly involved in pre-rRNA methylation, processing, and pre-ribosome assembly (Shubina *et al.*, 2016). However, it has been reported that in yeast and human cell fibrillarin is also a very dynamic and multifunctional protein executing functions in many different cellular processes. In addition to RNA processing, fibrillarin is implicated in DNA damage, abiotic stress, apoptosis, chromatin remodelling, and transcription mechanism. Moreover, to a large extent, its functional diversity is conferred upon by its interacting partner (Rodriguez-Corona *et al.*, 2015). Thus far, physiological functions of fibrillarin in plants are poorly understood. Several papers reported that the formation of ribonucleoproteins (RNP) between plant fibrillarin and viral RNAs is critical to protect the latter from the host defense system and to ensure systemic viral infection in plants (Kim *et al.*, 2007; Chang *et al.*, 2016). Arabidopsis FIB2 is primarily located in the nucleolus but also in the nucleoplasm (Loza-Muller *et al.*, 2015). Its presence in the nucleoplasm is consistent with the observation of Backstrom et al (2007) that FIB2 is recovered as MED36 subunit of the plant MEDIATOR complex. Here, we have confirmed these subcellular localizations of fibrillarin.

Analyses of KO mutants of FIB2 (*fib2-1* and *fib2-2*) showed that FIB2 is a negative regulator of expression of selective immune responsive genes, including *PR1*, after elf18 treatment (Fig. 2C to 2E). This molecular phenotype has been confirmed by the resistance phenotype against *Pst* DC3000 of *fib2* mutants (Fig. 2B). Our ChIP assays showed the occupancy of FIB2 directly on the *PR1* promoter and the release of this protein from the promoter region after elf18 treatment (Fig. 6). These results suggested that FIB2 functions as a repressor for *PR1* transcription. At this point, how FIB2 represses *PR1* expression remains unclear. In the case of

This article is protected by copyright. All rights reserved.

Accepted Article

yeast, it has been reported that fibrillarin, NOP1, could methylate a specific residue (Q105) of histone 2A (H2A) and alter the nucleosome structure of the rDNA locus by disrupting binding of the Facilitates Chromatin Transcription Complex (FACT), a histone chaperone involved in transcript elongation, to H2A. Being located only in the nucleolus, the function of NOP1 is restricted to the rDNA locus (Tessarz *et al.*, 2014). By contrast, the Arabidopsis FIB2 is also found outside of the nucleolus suggesting functions beyond the rDNA locus; moreover, it also has a conserved methyltransferase domain (Loza-Muller *et al.*, 2015). It is known that the FACT complex interacts with all three RNA polymerases and facilitates transcription by disrupting nucleosomes in the path of the polymerase and increasing the re-deposition of nucleosomes in the wake of transcribing polymerase (Hammond *et al.*, 2017). Besides, it has been reported that FACT accumulated on the *PR1* locus after SA treatment (Duroux *et al.*, 2004) suggesting that FACT could be involved in the transcriptional induction of *PR1*. Therefore, one possible explanation for the FIB2 repression mechanism is that this protein modifies histone H2A and regulates the occupancy of FACT complex on the *PR1* locus to alter its transcription.

We have previously identified ELENA1 and MED19a as positive regulators for *PR1* expression and shown that they likely function as a RNA/protein complex (Seo et al., 2017). Here, we found that in addition to MED19a ELENA1 also interacts with FIB2, a negative regulator. Although FIB2 has been reported to be associated with the Arabidopsis Mediator complex, MED subunits that bind to FIB2 have not yet been identified (Backstrom *et al.*, 2007). Our results here showed that FIB2 directly interacts with MED19a.

A general feature in transcriptional regulation of eukaryotes is the interaction between an activator and a repressor. One of the mechanisms of transcriptional activation is the removal the repressor from the activator by degradation (Perez & Goossens, 2013). Another mechanism is to dissociate the repressor/activator complex to enhance target gene transcription. To test whether ELENA1 regulates FIB2 protein stability, we examined FIB2 protein levels after elf18 treatment but found that they were not affected (Fig. 4B). We found that ELENA1 could release FIB2 from its interacting partner, MED19a, thus disrupting the FIB2/MED19a complex on the *PR1* promoter. This ‘eviction’ model is a known activating mechanism of lncRNA as has been described for X chromosome inactivation (XCI).

This article is protected by copyright. All rights reserved.

Accepted Article

At the pre-XCI stage, *Xist* is silenced by the binding of CCCTC-binding factor (CTCF) on its promoter. At the onset of XCI, a ncRNA transcript, *Jpx*, is up-regulated from both X chromosomes, which directly binds to CTCF and dissociates the latter from the *Xist* promoter. Then *Xist* expression allows the initiation of X-chromosome inactivation on one of the X chromosomes (Tian *et al.*, 2010; Sun *et al.*, 2013). Another example is the removal of polycomb repressive complexes (PRC2) by the ncRNA *Braveheart* during cardiovascular development. This ncRNA binds to the suppressor of Zeste 12 (SUZ12) subunit of PRC2 and releases the entire PRC2 complex from the chromosome (Klattenhoff *et al.*, 2013).

Although ELENA1 can interact with both MED19a and FIB2, it is not clear whether the interactions with both proteins are required for eviction of FIB2 from MED19a or binding of the lncRNA to either one of the two interacting proteins is sufficient to enhance *PR1* expression. Analysis of *med19a/fib2* double mutants showed that MED19a is required for transcriptional activation of *PR1* and its activity is blocked by FIB2 (Fig. 5A and 5B). Although *PR1* expression in the double mutant *med19a/fib2* is reduced as compared to *fib2,* it is still slightly higher than that in WT. Possible explanation for this modest difference in *PR1* expression is the presence of MED19b, a close homolog of MED19a, which may have redundant function. In our previous paper we have shown that ELENA1 could also bind to MED19b and *MED19b RNAi*/*med19a* transgenic line showed a further decrease in *PR1* expression (Seo *et al.,* 2017). Even if MED19a was depleted in the m19a/fib2 mutant, the remaining MED19b could still activate *PR1* expression. Therefore, the *PR1* expression results of *med19a/fib2* double mutants suggest that eviction of the FIB2 repressor from the mediator complex is also important for transcriptional activation. Results from these analyses also suggest that ELENA1 has an activation function for *PR1* expression in addition to removing the FIB2 repressor (Fig. 5C and 5D). On the other hand, overexpressing and inducible *ELENA1* transgenic plants showed that ELENA1 itself could not initiate *PR1* induction (Fig. 4D). This observation is consistent with the notion that ELENA1 could be involved in transcriptional elongation rather than the initiation process. The function of ELENA1 is to facilitate *PR1* expression after onset of t transcriptional induction by elf18 signal transduction.

This article is protected by copyright. All rights reserved.

Accepted Article

In conclusion, our studies show that after elf18 activation of the signaling cascade, ELENA1 is required to enhance the transcription of immune-responsive genes through interacting with transcriptional machinery components, including Mediator subunit and fibrillarin (Fig. 7). We anticipate that the interaction of lncRNAs and components of the transcription machinery may be a general regulatory theme. Further studies of other lncRNAs will uncover the additional complexity of lncRNAs in plant transcriptome regulation.

ACKNOWLEDGMENTS

This work was funded in part by a grant (NRF-RSSS-002) awarded by the National Research Foundation, Singapore.

AUTHOR CONTRIBUTIONS

J.S.S. and N-H.C. conceived the research plans; J.S.S and N-H.C. designed the experiments; J.S.S., P.D., and B.S.P. performed the experiments; J.S.S and N-H.C. wrote the article.

SUPPORTING INFORMATION

Fig. S1 Expression analyses of *fib2* knockout mutants and complemented lines.

Fig. S2 Expression analyses of *35S:FIB2-myc/WT* lines.

Fig. S3 Western blotting with native MED19a antibody.

Fig. S4 Gene expression analyses of *XVE:ELENA1/35S:FIB2-myc* lines and *XVE:ELENA1/WT* line.

Fig. S5 Full western blots in Fig. 4

Fig. S6 Gene expression level in transgenic lines used in Fig. 5.

Table S1. Primers used in this study

This article is protected by copyright. All rights reserved.

Accepted Article

Accepted Article

REFERENCES

Allen BL, Taatjes DJ. 2015. The Mediator complex: a central integrator of transcription. *Nature Reviews Molecular Cell Biology* **16**: 155-166.

Alonso JM, Stepanova AN, Leisse TJ, Kim CJ, Chen H, Shinn P, Stevenson D, Zimmerman J, Barajas P, Cheuk R et al. 2003. Genome-wide insertional mutagenesis of Arabidopsis thaliana. *Science* **301**(5633)**:** 653-657.

Backstrom S, Elfving N, Nilsson R, Wingsle G, Bjorklund S. 2007. Purification of a plant mediator from Arabidopsis thaliana identifies PFT1 as the Med25 subunit. *Molecular Cell* **26**: 717-729.

Bardou F, Ariel F, Simpson CG, Romero-Barrios N, Laporte P, Balzergue S, Brown JW, Crespi M. 2014. Long noncoding RNA modulates alternative splicing regulators in Arabidopsis. *Developmental Cell* **30**: 166-176.

Batista PJ, Chang HY. 2013. Cytotopic localization by long noncoding RNAs. *Current Opinion in Cell Biology* **25**: 195-199.

Bigeard J, Colcombet J, Hirt H. 2015. Signaling mechanisms in pattern-triggered immunity (PTI). *Molecular Plant* **8**: 521-539.

Boller T, Felix G. 2009. A renaissance of elicitors: perception of microbe-associated molecular patterns and danger signals by pattern-recognition receptors. *Annual Review of Plant Biology* **60**: 379-406.

Bourbon HM. 2008. Comparative genomics supports a deep evolutionary origin for the large, four-module transcriptional mediator complex. *Nucleic Acids Research* **36**: 3993-4008.

Bowler C, Benvenuto G, Laflamme P, Molino D, Probst AV, Tariq M, Paszkowski J. 2004. Chromatin techniques for plant cells. *Plant Journal* **39**: 776-789.

Cech TR, Steitz JA. 2014. The noncoding RNA revolution-trashing old rules to forge new ones. *Cell* **157**: 77-94.

This article is protected by copyright. All rights reserved.

Accepted Article

Chang CH, Hsu FC, Lee SC, Lo YS, Wang JD, Shaw J, Taliansky M, Chang BY, Hsu YH, Lin NS. 2016. The Nucleolar Fibrillarin Protein Is Required for Helper Virus-Independent Long-Distance Trafficking of a Subviral Satellite RNA in Plants. *Plant Cell* **28**: 2586-2602.

Chen LL. 2016. Linking Long Noncoding RNA Localization and Function. *Trends in Biochemical Science* **41**: 761-772.

Clough SJ, Bent AF. 1998. Floral dip: a simplified method for Agrobacterium-mediated transformation of Arabidopsis thaliana. *Plant Journal* **16**: 735-743.

Dolan WL, Chapple C. 2017. Conservation and Divergence of Mediator Structure and Function: Insights from Plants. *Plant & Cell Physiology* **58**: 4-21.

Duroux M, Houben A, Ruzicka K, Friml J, Grasser KD. 2004. The chromatin remodelling complex FACT associates with actively transcribed regions of the Arabidopsis genome. *Plant Journal* **40**: 660-671.

Franco-Zorrilla JM, Valli A, Todesco M, Mateos I, Puga MI, Rubio-Somoza I, Leyva A, Weigel D, Garcia JA, Paz-Ares J. 2007. Target mimicry provides a new mechanism for regulation of microRNA activity. *Nature Genetics* **39**: 1033-1037.

Furukawa T, Inagaki H, Takai R, Hirai H, Che FS. 2014. Two distinct EF-Tu epitopes induce immune responses in rice and Arabidopsis. *Molecular Plant-Microbe Interactions* **27**: 113-124.

Hammond CM, Stromme CB, Huang H, Patel DJ, Groth A. 2017. Histone chaperone networks shaping chromatin function. *Nature Reviews Molecular Cell Biology* **18**: 141-158.

Henriques R, Wang H, Liu J, Boix M, Huang LF, Chua NH. 2017. The antiphasic regulatory module comprising *CDF5* and its antisense RNA *FLORE* links the circadian clock to photoperiodic flowering. *New Phytologist* **216**: 854-867.

Heo JB, Sung S. 2011. Vernalization-mediated epigenetic silencing by a long intronic noncoding RNA. *Science* **331**: 76-79.

This article is protected by copyright. All rights reserved.

Accepted Article

Jansen RP, Hurt EC, Kern H, Lehtonen H, Carmo-Fonseca M, Lapeyre B, Tollervey D. 1991. Evolutionary conservation of the human nucleolar protein fibrillarin and its functional expression in yeast. *Journal of Cell Biology* **113**: 715-729.

Jin J, Liu J, Wang H, Wong L, Chua NH. 2013. PLncDB: plant long non-coding RNA database. *Bioinformatics* **29**: 1068-1071.

Jones JD, Dangl JL. 2006. The plant immune system. *Nature* **444**: 323-329.

Karimi M, Inze D, Depicker A. 2002. GATEWAY vectors for Agrobacterium-mediated plant transformation. *Trends in Plant Science* **7**: 193-195.

Katagiri F, Thilmony R, He SY. 2002. The Arabidopsis thaliana-pseudomonas syringae interaction. *Arabidopsis Book* **1**: e0039.

Kim DH, Sung S. 2017. Vernalization-Triggered Intragenic Chromatin Loop Formation by Long Noncoding RNAs. *Developmental Cell* **40**: 302-312 e304.

Kim SH, Macfarlane S, Kalinina NO, Rakitina DV, Ryabov EV, Gillespie T, Haupt S, Brown JW, Taliansky M. 2007. Interaction of a plant virus-encoded protein with the major nucleolar protein fibrillarin is required for systemic virus infection. *Proceedings of the National Academy of Sciences* **104**: 11115-11120.

Klattenhoff CA, Scheuermann JC, Surface LE, Bradley RK, Fields PA, Steinhauser ML, Ding H, Butty VL, Torrey L, Haas S, et al. 2013. Braveheart, a long noncoding RNA required for cardiovascular lineage commitment. *Cell* **152**: 570-583.

Kunze G, Zipfel C, Robatzek S, Niehaus K, Boller T, Felix G. 2004. The N terminus of bacterial elongation factor Tu elicits innate immunity in Arabidopsis plants. *Plant Cell* **16**: 3496-3507.

Lam MT, Li W, Rosenfeld MG, Glass CK. 2014. Enhancer RNAs and regulated transcriptional programs. *Trends in Biochemical Sciences* **39**(4): 170-182.

This article is protected by copyright. All rights reserved.

Accepted Article

Liu F, Marquardt S, Lister C, Swiezewski S, Dean C. 2010. Targeted 3' processing of antisense transcripts triggers Arabidopsis FLC chromatin silencing. *Science* **327**: 94-97.

Liu J, Jung C, Xu J, Wang H, Deng S, Bernad L, Arenas-Huertero C, Chua NH. 2012. Genome-wide analysis uncovers regulation of long intergenic noncoding RNAs in Arabidopsis. *Plant Cell* **24**(11): 4333-4345.

Liu J, Wang H, Chua NH. 2015. Long noncoding RNA transcriptome of plants. *Plant Biotechnology Journal* **13**: 319-328.

Long Y, Wang X, Youmans DT, Cech TR. 2017. How do lncRNAs regulate transcription? *Science Advances* **3**: eaao2110.

Loza-Muller L, Rodriguez-Corona U, Sobol M, Rodriguez-Zapata LC, Hozak P, Castano E. 2015. Fibrillarin methylates H2A in RNA polymerase I trans-active promoters in Brassica oleracea. *Frontiers in Plant Science* **6**: 976.

Perez AC, Goossens A. 2013. Jasmonate signalling: a copycat of auxin signalling? *Plant, Cell & Environment* **36**(12): 2071-2084.

Qin XF, Holuigue L, Horvath DM, Chua NH. 1994. Immediate early transcription activation by salicylic acid via the cauliflower mosaic virus as-1 element. *Plant Cell* **6**(6): 863-874.

Rodriguez-Corona U, Sobol M, Rodriguez-Zapata LC, Hozak P, Castano E. 2015. Fibrillarin from Archaea to human. *Biology of the Cell* **107**(6): 159-174.

Samanta S, Thakur JK. 2015. Importance of Mediator complex in the regulation and integration of diverse signaling pathways in plants. *Frontiers in Plant Science* **6**: 757.

Schonberger J, Hammes UZ, Dresselhaus T. 2012. In vivo visualization of RNA in plants cells using the lambdaN_{22} system and a GATEWAY-compatible vector series for candidate RNAs. *Plant Journal* **71**(1): 173-181.

Seo JS, Sun HX, Park BS, Huang CH, Yeh SD, Jung C, Chua NH. 2017. ELF18-INDUCED LONG-NONCODING RNA Associates with Mediator to Enhance

This article is protected by copyright. All rights reserved.

Expression of Innate Immune Response Genes in Arabidopsis. *Plant Cell* **29**: 1024-1038.

Seo, J.S. and Chua, N.H. 2017. Trimolecular Fluorescence Complementation (TriFC) Assay for Direct Visualization of RNA-Protein Interaction in planta. *Bio-protocol* **7**: e2579.

Shin JH, Chekanova JA. 2014. Arabidopsis RRP6L1 and RRP6L2 function in *FLOWERING LOCUS C* silencing *via* regulation of antisense RNA synthesis. *PLOS Genetics* **10**: e1004612.

Shubina MY, Musinova YR, Sheval EV. 2016. Nucleolar Methyltransferase Fibrillarin: Evolution of Structure and Functions. *Biochemistry (Moscow)* **81**: 941-950.

Soutourina J. 2018. Transcription regulation by the Mediator complex. *Nature Reviews Molecular Cell Biology* **19**: 262-274.

Sun S, Del Rosario BC, Szanto A, Ogawa Y, Jeon Y, Lee JT. 2013. Jpx RNA activates Xist by evicting CTCF. *Cell* **153**: 1537-1551.

Tessarz P, Santos-Rosa H, Robson SC, Sylvestersen KB, Nelson CJ, Nielsen ML, Kouzarides T. 2014. Glutamine methylation in histone H2A is an RNA-polymerase-I-dedicated modification. *Nature* **505**: 564-568.

Tian D, Sun S, Lee JT. 2010. The long noncoding RNA, Jpx, is a molecular switch for X chromosome inactivation. *Cell* **143**: 390-403.

Vance KW, Ponting CP. 2014. Transcriptional regulatory functions of nuclear long noncoding RNAs. *Trends in Genetics* **30**: 348-355.

Wang H, Chung PJ, Liu J, Jang IC, Kean MJ, Xu J, Chua NH. 2014. Genome-wide identification of long noncoding natural antisense transcripts and their responses to light in Arabidopsis. *Genome Research* **24**: 444-453.

Wang HV, Chekanova JA. 2017. Long Noncoding RNAs in Plants. *Advances in Experimental Medicine and Biology* **1008**: 133-154.

This article is protected by copyright. All rights reserved.

Accepted Article

Wu HW, Deng S, Xu H, Mao HZ, Liu J, Niu QW, Wang H, Chua NH. 2018. A noncoding RNA transcribed from the *AGAMOUS* (*AG*) second intron binds to CURLY LEAF and represses *AG* expression in leaves. *New Phytologist* **219**: 1480-1491

Zhang X, Henriques R, Lin SS, Niu QW, Chua NH. 2006. Agrobacterium-mediated transformation of Arabidopsis thaliana using the floral dip method. *Nature Protocol* **1**: 641-646.

Zipfel C, Kunze G, Chinchilla D, Caniard A, Jones JD, Boller T, Felix G. 2006. Perception of the bacterial PAMP EF-Tu by the receptor EFR restricts Agrobacterium-mediated transformation. *Cell* **125**: 749-760.

Accepted Article

This article is protected by copyright. All rights reserved.

Accepted Article

FIGURE LEGENDS

Fig. 1 ELF18-INDUCED LONG NONCODING RNA 1 (ELENA1) associates with FIBRILLARIN 2 (FIB2). (a) *In vitro* binding assay with *in vitro* transcribed (IVT) biotinylated ELENA1 RNA and recombinant maltose binding protein (MBP)-FIB2 protein. (b) *In vitro* binding competition assay with recombinant MBP-FIB2 protein and IVT ELENA1 RNA. (c) *In vitro* binding between FIB2-myc from nuclear extracts and IVT sense or anti-sense ELENA1 RNA. (d) Trimolecular fluorescence complementation (TriFC) assay in *Nicotiana benthamiana* leaves. nYFP was fused to FIB2, cYFP to MSCP and 6xMS2 nucleotide sequences to sense or anti-sense ELENA1. (d-i) and (d-ii) are negative control, and (d-iv) is magnified image of (d-iii) (C, chloroplast; N, nucleus; W, cell wall). Confocal images were taken 2 d after infiltration of *Agrobacterium* suspensions. Bars, 10 μm. (e) RNA immunoprecipitation (RIP) assay with *35S:FIB2-myc* line during elf18 treatment. Data (mean ± SD of qPCR; n = 3 independent seedling pools) are represented relative to the background level of RNA precipitation (*ACT2*). +RT, with reverse transcription of precipitates; –RT, without reverse transcription of immunoprecipitates. Asterisks indicate statistically significant difference compared with 0 h. **, $P < 0.01$ (two-tailed t-test). For (a, b), MBP was used as a negative control.

Fig. 2 Defense phenotype of *fibrillarin 2* (*fib2*) mutants. (a) Schematic diagram (upper panel) of T-DNA insertion sites and SALK line numbers in Arabidopsis *fib2* knock-out mutants (*fib2-1* and *fib2-2*). Diagram (lower panel) represents domains of FIB2, and the numbers refer to amino acid positions. GAR, glycine arginine-rich domain; SP, space domain; AHR, alpha helix-rich domain. (b) The growth of *Pseudomonas syringae* pv *Tomato* (*Pst*) DC3000 in plants of various Arabidopsis genotypes, Col-0 (WT), *fib2-1*, and *fib2-2* lines were inoculated with *Pst* DC3000, and bacterial population in each was determined at 4 d post-inoculation. Bars indicate ± SD (n = 3 independent plants). CFU, colony-forming units. Time course of (c) *PATHOGENESIS-RELATED GENE 1* (*PR1*), (d) *CYTOCHROME P450, FAMILY 82, SUBFAMILY C, POLYPEPTIDE* 2 (CYP82C2), and (e) *ACIREDUCTONE DIOXYGENASE 3* (*ARD3*) expression after elf18 treatment in the Col-0, *fib2-1*, and

This article is protected by copyright. All rights reserved.

fib2-2. (c–e) Transcript levels were normalized to *ACT2* expression levels, and bars represent average ± SD (*n* = 3 independent seedling pools). *Y*-axis shows relative values compared to the wild-type (WT) expression level without treatment. (b–e) Asterisks indicate statistically significant difference compared with WT (Col-0) as analysed by one-way ANOVA followed by t-test: **, $P < 0.01$.

Fig. 3 FIBRILLARIN 2 (FIB2) interacts with Mediator subunit 19a (MED19a). (a) *In vitro* pull-down assay to explore the possible interaction between MED19a and FIB2. Maltose binding protein (MBP) and Mediator subunit 28 (MED28) were used as negative controls. (b) Yeast two-hybrid assay with FIB2 and MED19a. FIB2 was fused with GAL4 binding domain (BD), and MED19a was fused with GAL4 activating domain (AD). Empty vector and MED28 were used as negative controls. (c) Co-immunoprecipitation (Co-IP) result of *35S:FIB2-myc* plants (Arabidopsis). IP with myc antibody and western blotting with MED19a antibody. Two independent transgenic lines were analyzed. (d) Bimolecular fluorescence complementation (BiFC) analysis of interaction between FIB2 and MED19a in tobacco cells. (d-i) and (d-ii) are negative control, and (d-iv) is magnified image of (d-iii). Reconstituted YFP signals were detected in nuclei of tobacco leaf cells when nYFP-MED19a was transiently coexpressed with FIB2-cYFP in *Nicotiana benthamiana* leaves infiltrated with *Agrobacterium* suspensions. Confocal images were taken 2 d after infiltration. Bars, 10 μm.

Fig. 4 ELF18-INDUCED LONG NONCODING RNA 1 (ELENA1) dissociates the Mediator subunit 19a (MED19a)/ FIBRILLARIN 2 (FIB2) complex. (a) *In vitro* pull-down assay of glutathione S-transferase (GST)-MED19a and MBP-FIB2 with *in vitro* transcribed (IVT) ELENA1 RNA (left) and GFP mRNA (right). RNA amount was given as ng μl^{-1}. (b) *In vivo* time course co-immunoprecipitation (Co-IP) assay using *35S:FIB2-myc* plants (Arabidopsis) after elf18 treatment. IP with myc antibody and western blotting with MED19a antibody. Two independent transgenic lines were analyzed. (c) *In vivo* time course Co-IP assays in *XVE:ELENA1/35S:FIB2-myc* plants (Arabidopsis) after 20 μM beta-estradiol treatment. IP with anti-c-myc antibody and western blotting with MED19a antibody. Two independent transgenic lines were

This article is protected by copyright. All rights reserved.

Accepted Article

analyzed. We performed each experiment three times with independent seedling pools. Full blots were shown in Supporting Information Fig. S5.

Fig. 5 *PATHOGENESIS-RELATED GENE 1* (*PR1*) expression in *FIBRILLARIN 2* (*FIB2*) and *Mediator subunit 19a* (*MED19a*) (or *ELF18-INDUCED LONG NONCODING RNA 1* (*ELENA1*)) double mutants. (a) *PR1* expression in *med19a-2/fib2-1* (m19a/fib2) plant. m19a is *med19a-2* and fib2 is *fib2-1*. (b) *PR1* expression in *35S:GFP-MED19a*/*fib2-1* (M19a/m36a) plants. M19a#1 is *35S:GFP-MED19a-1*. (c) *PR1* expression in *ELENA1 KD-10*/*fib2-1* (e1#10/fib2) plants. (d) *PR1* expression in *35S:ELENA1*/*fib2-1* (E1/fib2) plants. All the transgenic lines were generated with Arabidopsis. All gray bars are values for mock treatment (without elf18) and black bars are values for 18 h 1 μM elf18 treatment. *Y*-axis shows relative values compared to the wild-type (WT) expression level without treatment. Bars represent average ± SD (*n* = 3 independent seedling pools). Asterisks indicate statistically significant difference compared with WT or between indicated values as analysed by one-way ANOVA followed by *t*-test: *, $P < 0.05$; **, $P < 0.01$.

Fig. 6 FIBRILLARIN 2 (FIB2) enrichment on the *PATHOGENESIS-RELATED GENE 1* (*PR1*) promoter. (a) A schematic diagrams of the *PR1* promoter (2460 bp) and the five different regions (P1–P5) used for chromatin immunoprecipitation (ChIP) analysis. P4 region includes the *AS-1* cis-element (Qin *et al.*, 1994). (b) Time course of ChIP qPCR results of P_{FIB2}*:FIB2-GFP* line after elf18 treatment. ChIP signal in each region of the *PR1* promoter at each time point was quantified by qPCR. Numbers on the *x*-axis indicate positions of the PCR-amplified sites shown in panel A. (c) Relative enrichment of FIB2 on *PR1* promoter in P_{FIB2}*:FIB2-GFP*/*ELENA1* KD-10 and P_{FIB2}*:FIB2-GFP*/*ELENA1* OX-16 were shown in different times after 1 μM elf18 treatment. All the transgenic lines for ChIP assay were generated with Arabidopsis. Error bars indicate ± SD (*n* = 3 independent seedling pools). Asterisks indicate statistically significant difference compared with 0 h or between indicated values (b) and wild-type (WT) (Col-0) or between indicated values (c) as analysed by one-way ANOVA followed by *t*-test: *, $P < 0.05$; **, $P < 0.01$.

This article is protected by copyright. All rights reserved.

Accepted Article

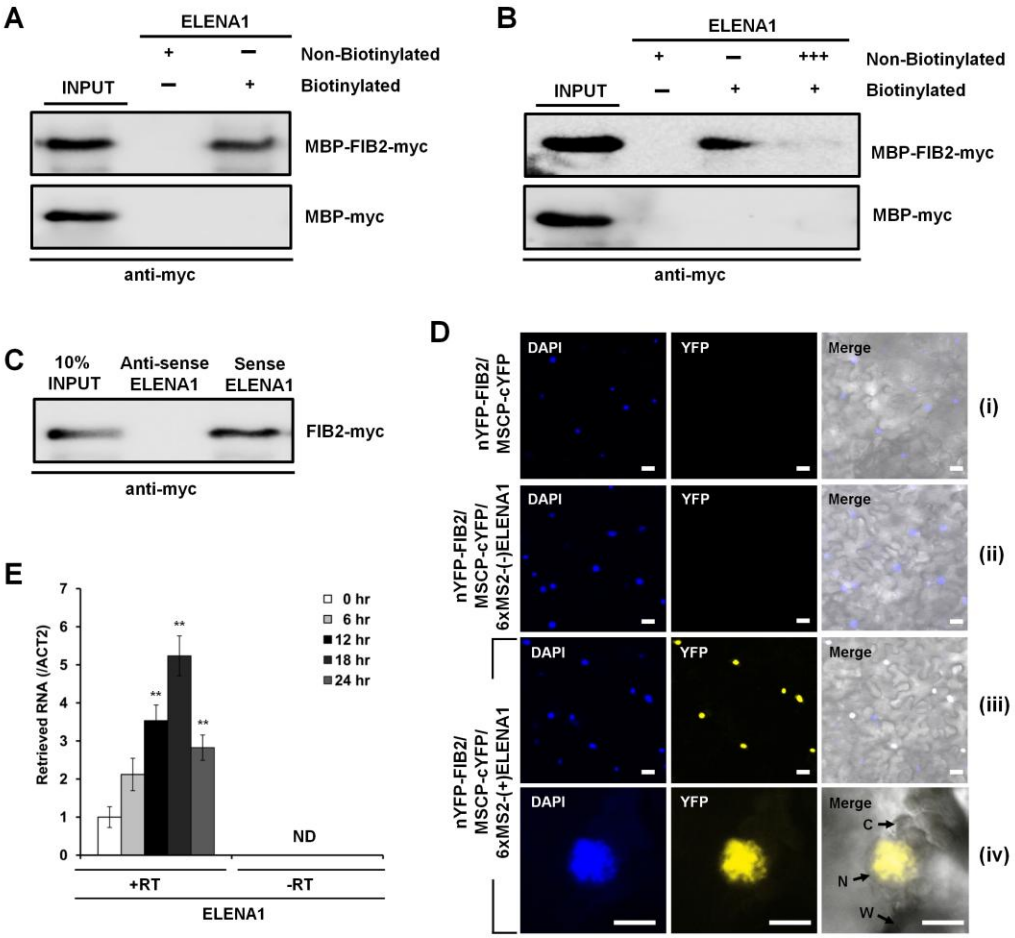
Fig. 7 Proposed mode of action. In the absence of pathogen-associated molecular pattern (PAMP) signaling (before treatment), FIBRILLARIN2 (FIB2) represses *PATHOGENESIS-RELATED GENE1* (*PR1*) expression either directly by histone modification or indirectly by inhibiting (blue) the action of Mediator subunit 19a (MED19a). After initiating PAMP signaling by EF-Tu RECEPTOR (EFR) receptor (after treatment), ELF18-INDUCED LONG NONCODING RNA 1 (ELENA1) transcript level increases (green) and binds to MED19a and FIB2. FIB2 is then evicted from the mediator complex, and MED19a remains on the promoter to activate (red) *PR1* expression.

Accepted Article

This article is protected by copyright. All rights reserved.

Accepted Article

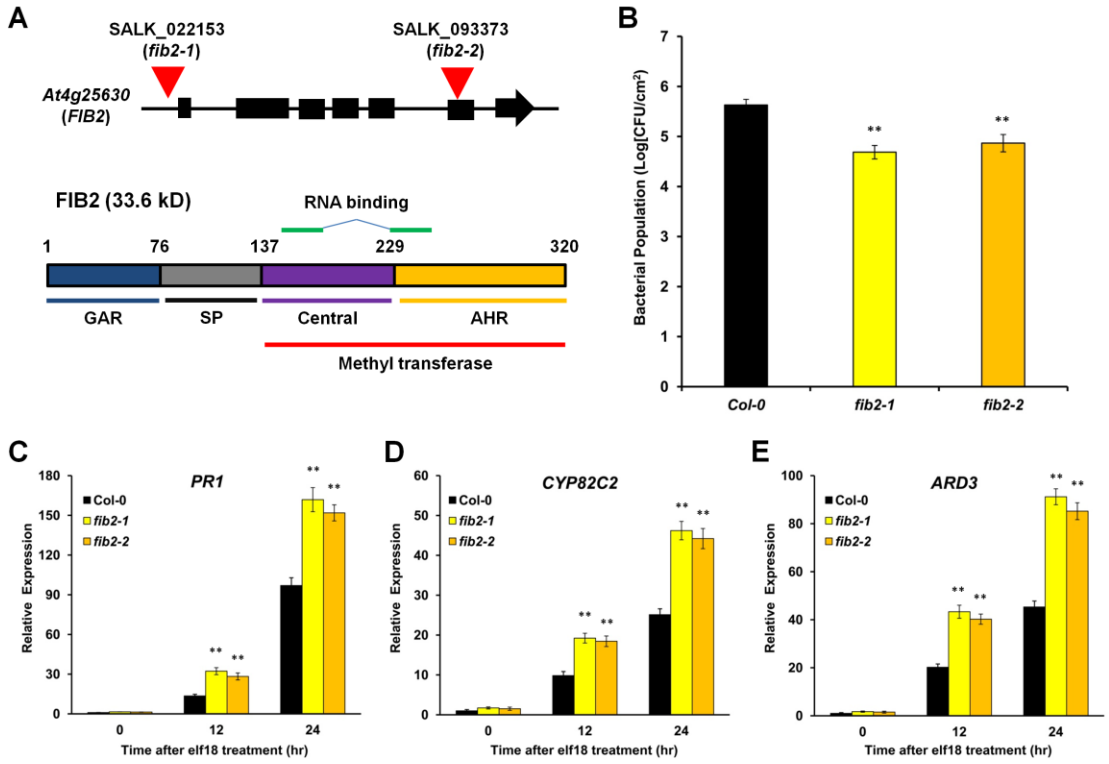
Figure 1



This article is protected by copyright. All rights reserved.

Accepted Article

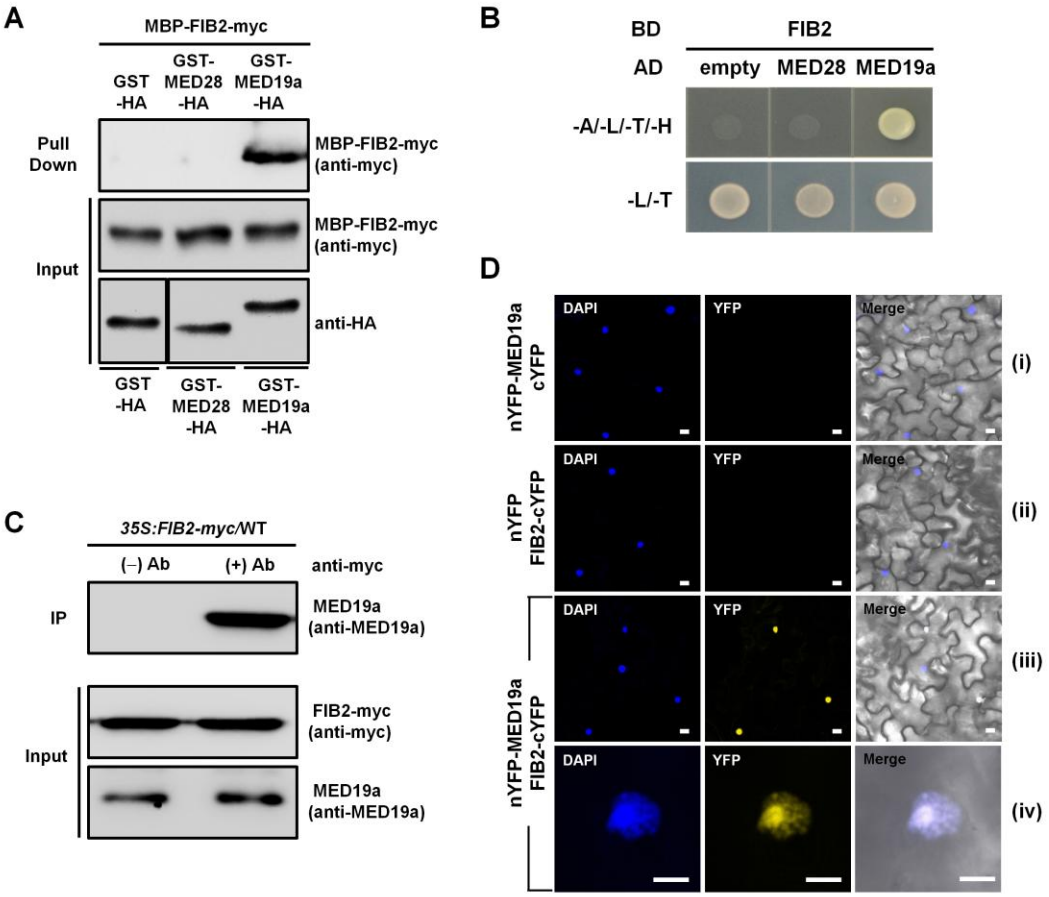
Figure 2



This article is protected by copyright. All rights reserved.

Accepted Article

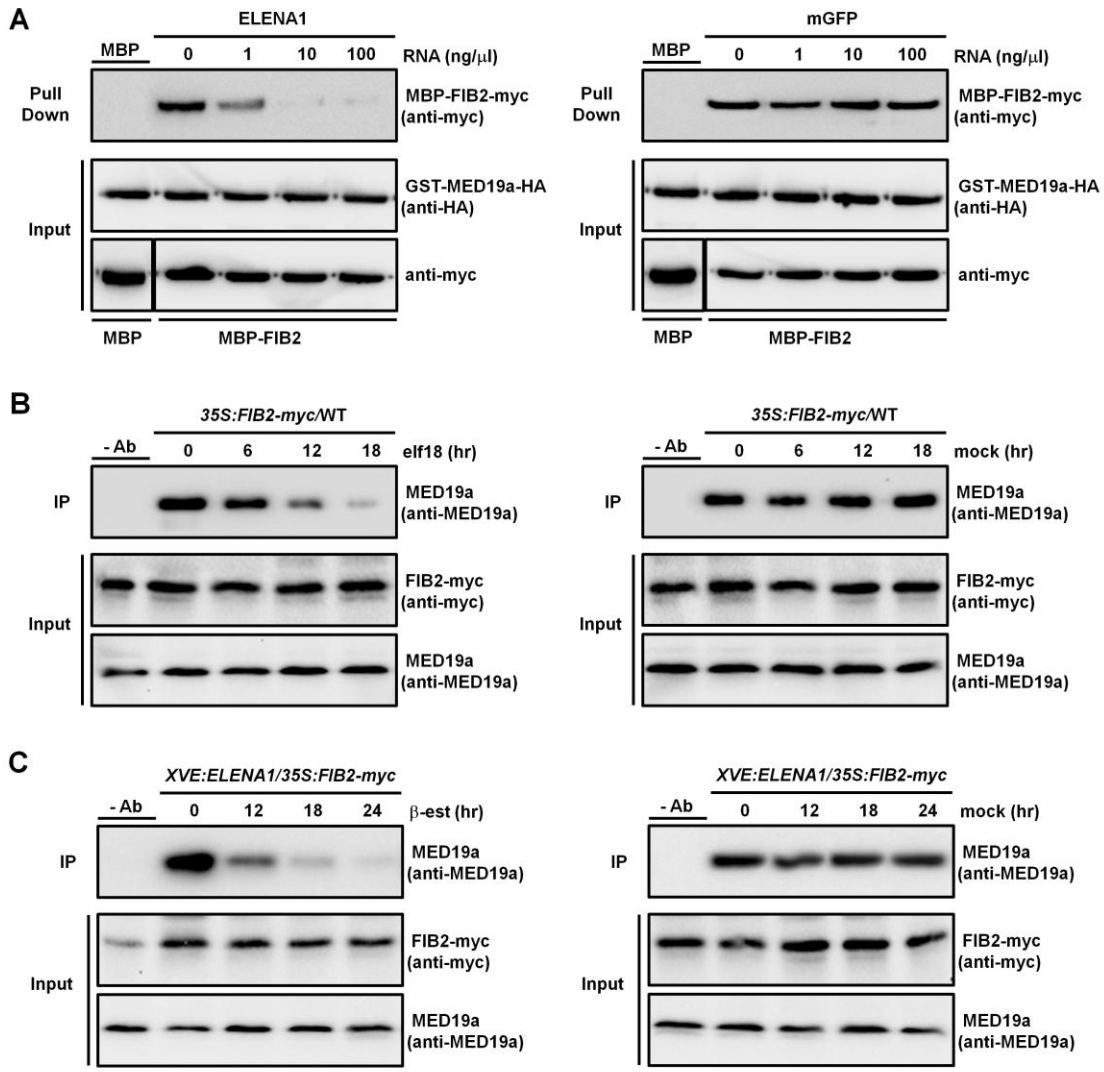
Figure 3



This article is protected by copyright. All rights reserved.

Accepted Article

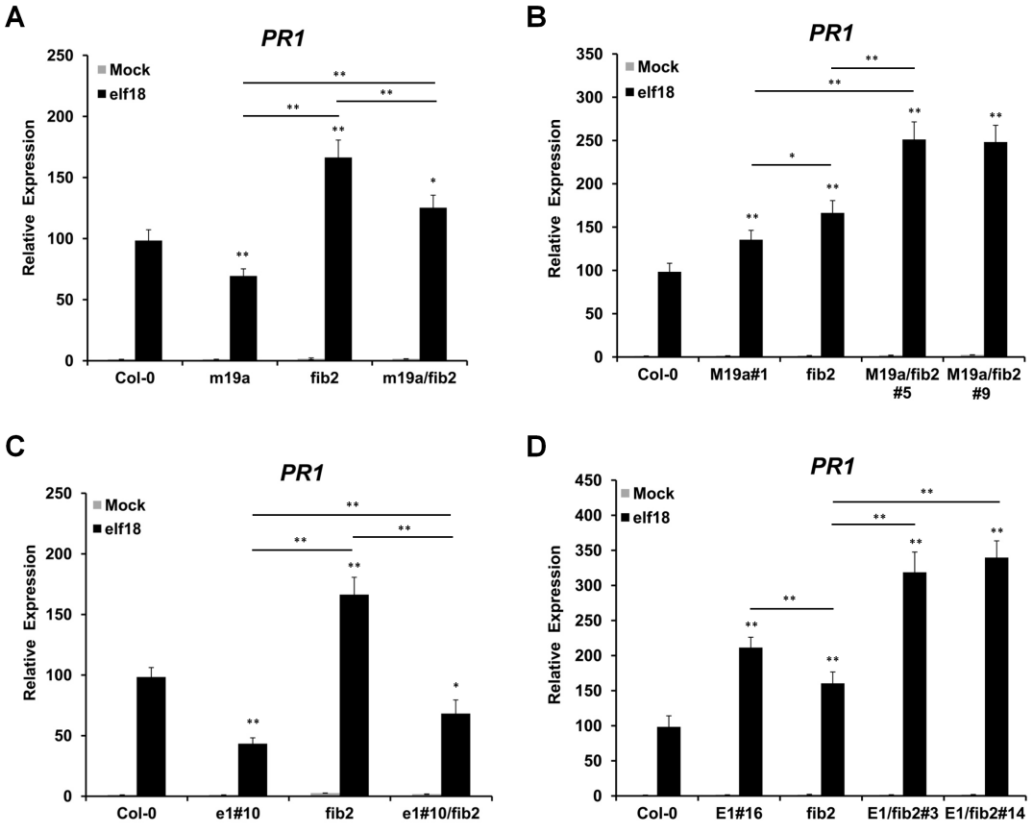
Figure 4



This article is protected by copyright. All rights reserved.

Accepted Article

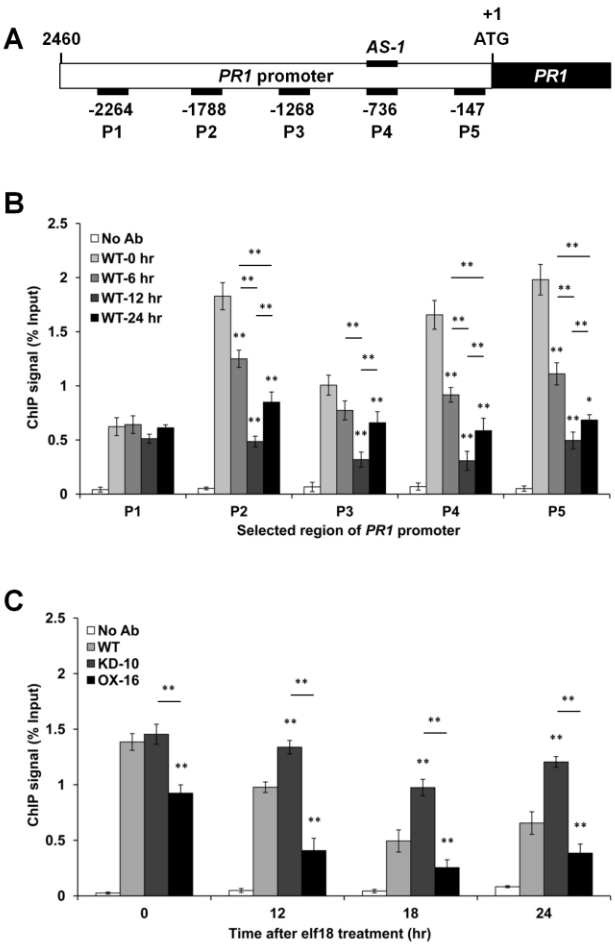
Figure 5



This article is protected by copyright. All rights reserved.

Accepted Article

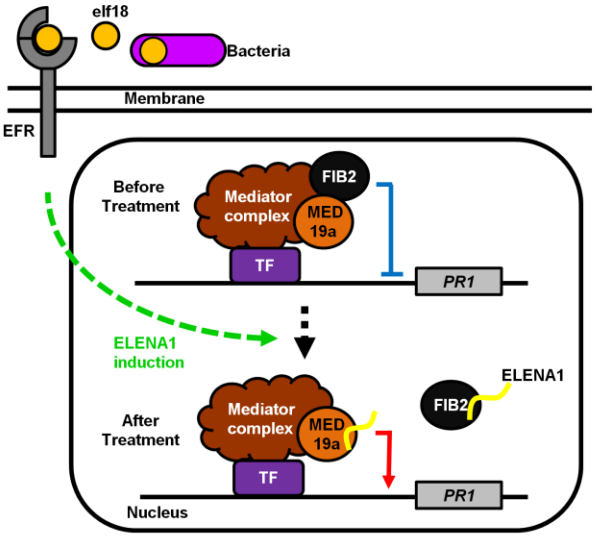
Figure 6



This article is protected by copyright. All rights reserved.

Accepted Article

Figure 7



This article is protected by copyright. All rights reserved.